Viable offspring derived from single unfertilized mammalian oocytes

Yanchang Wei[a,b,1] , Cai-Rong Yang[a,b,c], and Zhen-Ao Zhao[a,b,d]

[a]Center for Reproductive Medicine, Ren Ji Hospital, School of Medicine, Shanghai Jiao Tong University, Shanghai 200135, China; [b]Shanghai Key Laboratory for Assisted Reproduction and Reproductive Genetics, Shanghai 200135, China; [c]Center for Reproductive Sciences, University of California, San Francisco, CA 94143; and [d]State Key Laboratory of Stem Cell and Reproductive Biology, Institute of Zoology, Chinese Academy of Sciences, Beijing 100101, China

In mammals, a new life starts with the fusion of an oocyte and a sperm cell. Parthenogenesis, a way of generating offspring solely from female gametes, is limited because of problems arising from genomic imprinting. Here, we report live mammalian offspring derived from single unfertilized oocytes, which was achieved by targeted DNA methylation rewriting of seven imprinting control regions. Oocyte coinjection of catalytically inactive Cas9 (dCas9)-Dnmt3a or dCpf1-Tet1 messenger RNA (mRNA) with single-guide RNAs (sgRNAs) targeting specific regions induced de novo methylation or demethylation, respectively, of the targeted region. Following parthenogenetic activation, these edited regions showed maintenance of methylation as naturally established regions during early preimplantation development. The transfer of modified parthenogenetic embryos into foster mothers resulted in significantly extended development and finally in the generation of viable full-term offspring. These data demonstrate that parthenogenesis can be achieved by targeted epigenetic rewriting of multiple critical imprinting control regions.

oocyte | mammal | offspring | early embryo | genomic imprinting

In mammals, a new life begins with the sperm successfully meeting the oocyte. Parthenogenesis, a way of generating offspring solely from unfertilized oocytes, is limited in mammals because of problems arising from genomic imprinting (1, 2). Although bimaternal mice constructed with a nongrowing (ng) oocyte, which mimics the paternal genome, and a fully grown oocyte have been generated by genetic manipulation of specific imprinting regions (3, 4), the use of the ng oocyte derived from newborn mice limits the application of this method. Parthenogenetic offspring, in which an individual develops from a single unfertilized oocyte, have not been reported in mammals.

Fine coordination between the paternal and the maternal genomes is essential for mammalian development (5–8). However, this coordination is disrupted in parthenogenetic embryos because of the 2-fold establishment of the maternal-specific imprinting of the diploid genome. Several paternally methylated imprinting control regions (ICRs), including the H19 (9) and Gtl2 (10) ICRs, function in the regulation of genes that are essential for embryonic development. Several maternally methylated ICRs, such as Igf2r (11), Snrpn (12), Kcnq1ot1 (13), Nespas (14), and Peg10 (15) ICRs, have been shown to play pivotal roles in the regulation of fetal and/or postnatal growth and development. In addition, some studies have identified several imprinting regions that are critical for supporting the full-term development of bimaternal and bipaternal embryos (16, 17).

In this study, we examined whether the targeted epigenetic rewriting of these regions could improve parthenogenetic development. By the targeted methylation editing of seven ICRs, we were able to generate viable full-term offspring directly from single unfertilized mouse oocytes.

Results and Discussion

Because previous evidence demonstrated that two paternally methylated ICRs, the H19 and Gtl2 ICRs, form the major barrier that prevents bimaternal embryos from full-term development (3, 4), we first asked whether the targeted methylation rewriting of these two ICRs could improve parthenogenetic development. We used a strategy that can achieve targeted methylation editing of the imprinting region of one allele but not the other. We employed B6CASTF1 (C57BL/6 ♀ × CAST ♂) background mice, which carry sufficient single-nucleotide polymorphisms (SNPs) for specific targeting. We designed single-guide RNAs (sgRNAs) with a protospacer adjacent motif (PAM) region that matches one allele but not the other (Fig. 1A). We coinjected catalytically inactive Cas9 (dCas9)-Dnmt3a messenger RNA (mRNA) and sgRNAs targeting both H19 and Gtl2 ICRs into germinal vesicle (GV) oocytes (SI Appendix, Table S1, which includes all of the guide RNAs [gRNAs] used in this study) and determined the editing effects by bisulfite sequencing of single metaphase of the second meiosis (MII) oocytes using a protocol previously developed in our laboratory (18), which enables the simultaneous detection of methylation of a specific region of a single-oocyte nucleus and its sibling first polar body (PB1) with high efficiency. Bisulfite sequencing showed that the majority of alleles from the C57BL/6 background were hypermethylated at the H19 ICR, whereas nearly all of the alleles from the CAST background were hypomethylated at the H19 ICR, indicating the successful de novo methylation of the H19 ICR on one allele but not the other (Fig. 1B and SI Appendix, Fig. S1). We used a similar strategy to validate the allele-specific de novo methylation of the Gtl2 ICR. Gtl2 contains an ∼4.15-kb ICR that regulates imprinting of an ∼1-Mb cluster of genes due to allele-specific

Significance

In mammals, parthenogenesis is limited because of problems arising from genomic imprinting. Here, we report live mammalian offspring derived from single unfertilized eggs. This was achieved by the targeted DNA methylation rewriting of seven imprinting control regions. By designing guide RNAs with protospacer adjacent motif (PAM) sequences matching one allele but not the other, dCas9-Dnmt3a or dCpf1-Tet1 enables targeted DNA methylation editing in an allele-specific manner. The success of parthenogenesis in mammals opens many opportunities in agriculture, research, and medicine.
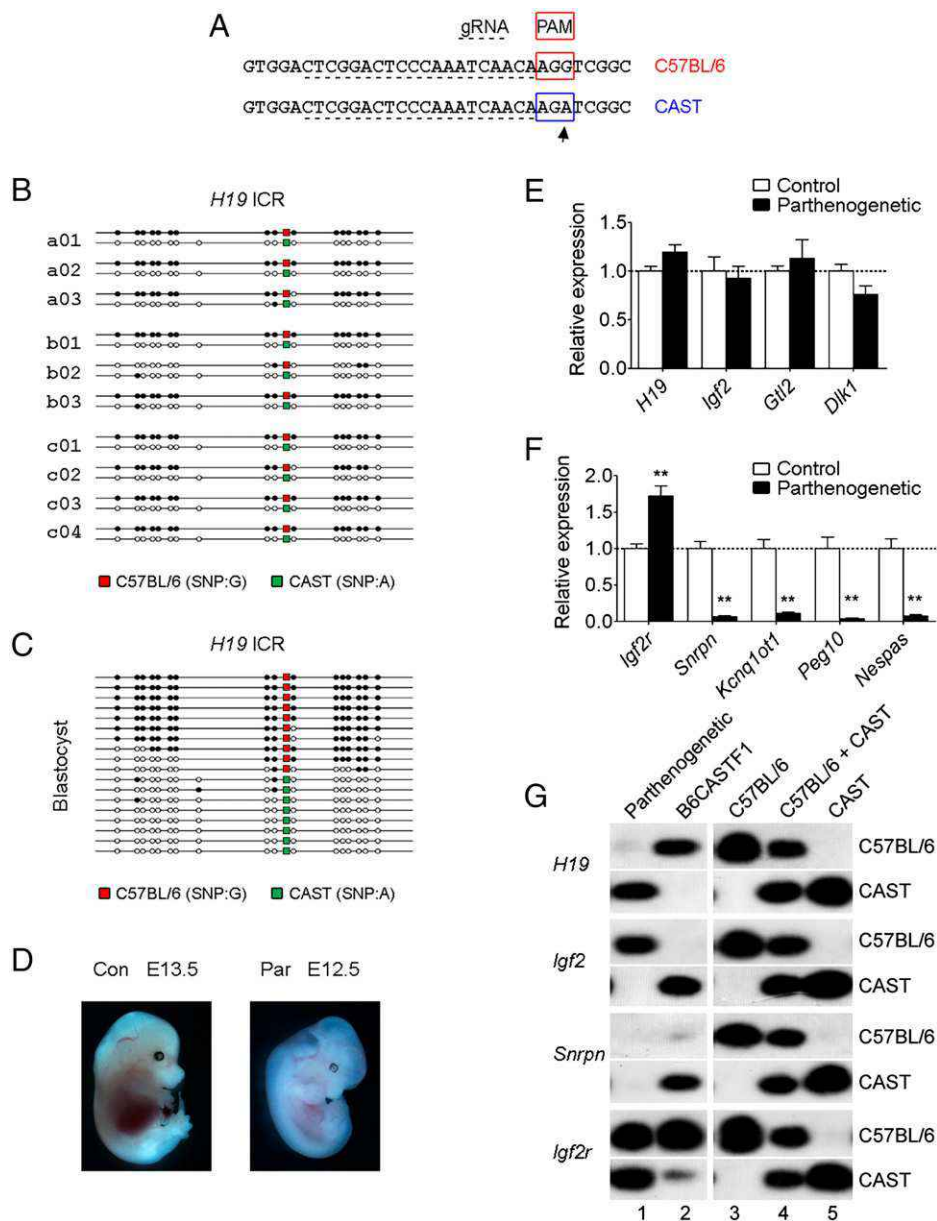
DEVELOPMENTAL BIOLOGY

Fig. 1. Targeted DNA methylation rewriting of *H19* and *Gtl2* ICRs in parthenogenetic embryos. (*A*) Strategy to target one allele but not the other. The sgRNA sequence is underlined. The PAM for sgRNA (NGG) is labeled by a red box. The arrow indicates the SNP (C57BL/6, G; CAST, A). (*B*) Targeted de novo methylation of the *H19* ICR on the C57BL/6 allele in oocytes. Single MII oocytes were subjected to bisulfite sequencing analysis. Each single-oocyte sample was assigned an ID beginning with a letter, followed by a two-digit number. Different letters represent different oocyte donors, and different numbers distinguish different oocytes from the same donor. White circles represent unmethylated CpGs dinucleotides (CpGs), and black circles represent methylated CpGs. The polymorphism is indicated with red for G from the C57BL/6 allele and with green for A from the CAST allele. Two additional regions for *H19* are in *SI Appendix*, Fig. S1. The editing of the *Gtl2* ICR methylation is present in *SI Appendix*, Fig. S2. (*C*) Maintenance of methylation of the *H19* ICR in parthenogenetic preimplantation embryos. A schematic representation of the construction of putatively diploid parthenogenetic embryos is shown in *SI Appendix*, Fig. S6A. After parthenogenetic activation and in vitro embryonic culture, one-third of the converted DNA from 30 to 40 pooled E 3.5 blastocysts was subjected to bisulfite sequencing analysis. Two additional regions for *H19* are present in *SI Appendix*, Fig. S6B. The maintenance of methylation of the *Gtl2* ICR is present in *SI Appendix*, Fig. S6C. (*D*) Fetuses at 13.5 d derived from control fertilized embryos (left). No modified parthenogenetic embryos developed to 13.5 d, and shown is the most advanced fetus at 12.5 d derived from modified parthenogenetic embryos (right). (*E*) Quantitative real-time PCR analysis of imprinted genes regulated by paternally methylated ICRs in control (white columns) and reconstructed parthenogenetic (black columns) E 9.5 embryos. (*F*) Quantitative real-time PCR analysis of imprinted genes regulated by maternally methylated ICRs in control (white columns) and reconstructed parthenogenetic (black columns) E 9.5 embryos. Control, $n = 9$; parthenogenetic, $n = 10$. The values represent expression levels relative to that of the internal control gene *Gapdh*. Data are expressed as mean ± SEM *$P < 0.05$, **$P < 0.01$, versus control. The dotted line (set as 1) represents the average of expression levels of each gene from controls. (*G*) SNuPE assays for allele-specific expression of the indicated genes. Lanes 1 and 2 contained DNA derived from the pooled RNA of reconstructed parthenogenetic and fertilized control E 9.5 embryos, respectively. Lanes 3 and 5 contained DNA derived from the pooled RNA of C57BL/6 and CAST E 9.5 embryos, respectively. Lane 4 contained DNA derived from a 1:1 mixture of RNA from C57BL/6 and CAST E 9.5 embryos.

methylation (10). Four sgRNAs were designed to target this locus, and three regions dispersed on the ICR were used for methylation analysis to validate the targeting effect. The majority of alleles from the C57BL/6 background showed hypermethylation at these three regions, suggesting the potentially successful allele-specific methylation editing of the *Gtl2* ICR (*SI Appendix*, Fig. S2). The effective targeting range of this system can be over 500 bp on both sides of the gRNA targeting site but does not extend past 1,000 bp on either side (*SI Appendix*, Fig. S3). Thus, designing multiple sgRNAs within a target locus with an appropriate interval would provide effective editing efficiency and high specificity that, furthermore, would not be expected to extend to promoters of neighboring genes. Replacing either sgRNA with scrambled sgRNA or Dnmt3a with an inactive form resulted in no induction, excluding the possibility of Dnmt3a overexpression or small RNA introduction (*SI Appendix*, Fig. S4). Off-target analysis of the three most likely off-target loci showed no significant changes in methylation, suggesting the potentially high specificity of this system (*SI Appendix*, Fig. S5). After parthenogenetic activation and in vitro embryonic culture, these parthenogenetic embryonic day (E) 3. 5 blastocysts exhibited hypermethylation on both *H19* and *Gtl2* ICRs derived from the C57BL/6 background allele but hypomethylation of the allele derived from the CAST background, suggesting the maintenance of methylation during preimplantation development (Fig. 1*C* and *SI Appendix*, Fig. S6). Next, we transferred modified parthenogenetic E 3.5 blastocysts[H19me+Gtl2me+] into CD1 foster mothers. However, we did not obtain development of full-term offspring, as evidenced by the majority of embryos dying before E 12.5 (Fig. 1*D*). Quantitative real-time PCR analysis revealed largely normal expression of the imprinted genes regulated by the two paternally methylated ICRs, *H19* and *Gtl2* (Fig. 1*E*), but abnormal expression of the imprinted genes regulated by maternally methylated ICRs (Fig. 1*F*). Allele-specific expression was measured by single-nucleotide primer extension (SNuPE) after RT-PCR (19, 20). Parthenogenetic embryos with both ICRs edited showed largely monoallelic expression of *H19* and *Igf2* (Fig. 1*G*, lane 1), which is similar to the monoallelic expression seen in the fertilized control embryos (Fig. 1*G*, lane 2). In contrast, these embryos exhibited no expression of either allele of *Snrpn*, which is normally expressed only from the paternal allele, and biallelic expression of *Igf2r*, which is normally expressed only from the maternal allele (Fig. 1*G*). The *H19* ICR contains four methylation-sensitive CTCF binding sites, which are critical for regulating imprinting of this imprinting cluster (*SI Appendix*, Fig. S1*A*, which shows schematic representation of the *H19* ICR with information on four CTCF binding sites within it) (21). To determine whether methylation editing alters CTCF binding, we performed a CTCF chromatin immunoprecipitation (ChIP) assay at these four loci. The binding of CTCF to the four targeted sites was comparable in samples from modified parthenogenetic embryos and in samples from naturally fertilized embryos (*SI Appendix*, Fig. S7), suggesting returned CTCF binding as a result of methylation editing.

We then turned our attention to maternally methylated ICRs. We selected five maternally methylated ICRs whose abnormalities have been linked to embryonic or postnatal lethality or severe developmental disorders (22). These were *Igf2r* (11), *Snrpn* (12), *Kcnq1ot1* (13), *Nespas* (14), and *Peg10* (15) ICRs (*SI Appendix*, Table S1, which summarizes all of the ICRs targeted, as well as all of the gRNAs used in this study). Quantitative real-time PCR analysis revealed that the imprinted genes regulated by these five ICRs were abnormally expressed as described above (Fig. 1*F*). We asked whether targeted editing of methylation of these five ICRs, together with *H19* and *Gtl2* ICRs, could further improve parthenogenetic development. To achieve targeted demethylation of one allele but not the other, we used dCpf1-Tet1, which utilizes

TTN as the PAM (23), and designed sgRNAs with PAM sequences that matched one allele but not the other (Fig. 2*A*). We coinjected dCpf1-Tet1 mRNA with sgRNAs targeting these five regions into GV oocytes and evaluated the editing effect in both MII oocytes and parthenogenetic E 3.5 blastocysts. Single-oocyte bisulfite sequencing showed that in the majority of oocytes, one allele was hypomethylated, whereas the other remained hypermethylated, demonstrating the success of editing using this system (Fig. 2*B* and *SI Appendix*, Fig. S8). Moreover, after activation and in vitro embryonic culture, these edited marks showed maintenance of methylation during preimplantation development, similar to naturally established marks (Fig. 2*C* and *SI Appendix*, Fig. S9). The editing range of this system can be over 500 bp on both sides of the target sequence (*SI Appendix*, Fig. S10 *A* and *B*). In contrast, a gRNA ~1,200 bp upstream of the analyzed region induced only partial demethylation (*SI Appendix*, Fig. S10*C*). Designing multiple sgRNAs with an interval of less than 1,000 bp could effectively demethylate the target locus. The replacement of sgRNAs with scrambled sgRNAs or Tet1 with its inactive form did not show any induction, excluding that this effect was due to the overexpression of Tet1 or the introduction of small RNA (*SI Appendix*, Fig. S11). Off-target analysis of three candidate loci showed no significant off-target activity, suggesting the potentially high specificity of this system (*SI Appendix*, Fig. S12).

Next, to determine whether simultaneous modification of two paternally methylated ICRs via dCas9-Dnmt3a and five maternally methylated ICRs via dCpf1-Tet1, as mentioned above, could further extend development, we constructed parthenogenetic embryos with all seven regions modified (*SI Appendix*, Fig. S13 for schematic). Quantitative real-time PCR of genes regulated by these ICRs revealed significantly improved expression in parthenogenetic E 9.5 embryos (Fig. 2 *D* and *E*). The SNuPE assay showed largely monoallelic expression of *H19*, *Igf2*, *Snrpn*, and *Igf2r* (Fig. 2*F*, lane 1) in these modified embryos, which is similar to the monoallelic expression pattern seen in the fertilized control embryos (Fig. 2*F*, lane 2). After transfer of 158 E 3.5 blastocysts into 12 pseudopregnant foster female mice, we were able to obtain 13 viable fetuses from three females at E 13.5, as evidenced by clear heartbeats. These data suggest that further methylation editing significantly improved parthenogenetic development. Of these 13 embryos, we selected 6 for methylation analysis of all seven ICRs edited in each single embryo. Bisulfite genomic sequencing revealed that two embryos possessed largely normal methylation patterns at all seven edited ICRs, whereas the remaining four displayed abnormal methylation in various ICRs, and each had at least one ICR (*SI Appendix*, Fig. S14). These data suggest that only a portion of embryos can be simultaneously successfully edited at all seven ICRs.

In the next series of experiments, we constructed parthenogenetic embryos with two paternally methylated ICRs and five maternally methylated ICRs modified, which we designated parthenogenetic embryos[2+5]; transferred E 3.5 blastocysts into foster mothers; and allowed them to develop to term. A total of 389 modified embryos[2+5] were constructed by micromanipulation. After artificial activation, 227 (58.4%) putatively parthenogenetic diploid one-cell embryos that formed two pronuclei and second polar bodies were recovered. After in vitro embryonic culture, 192 (84.6%) developed to the blastocyst stage and were transferred into 14 recipient females. A total of three (1.6%) pups were recovered by autopsy at 19.5 d of gestation (Table 1). Two of these pups had lower body weight (0.783 and 0.832 g) and showed slight growth retardation at birth; these pups died within 24 h. The remaining pup had body weight (1.101 g) similar to that of the wild type (1.147 ± 0.042 g; mean ± SEM) and grew to adulthood (Fig. 3*A*). Bisulfite sequencing of tail tissue derived from the surviving mouse demonstrated that all edited ICRs exhibited correct methylation
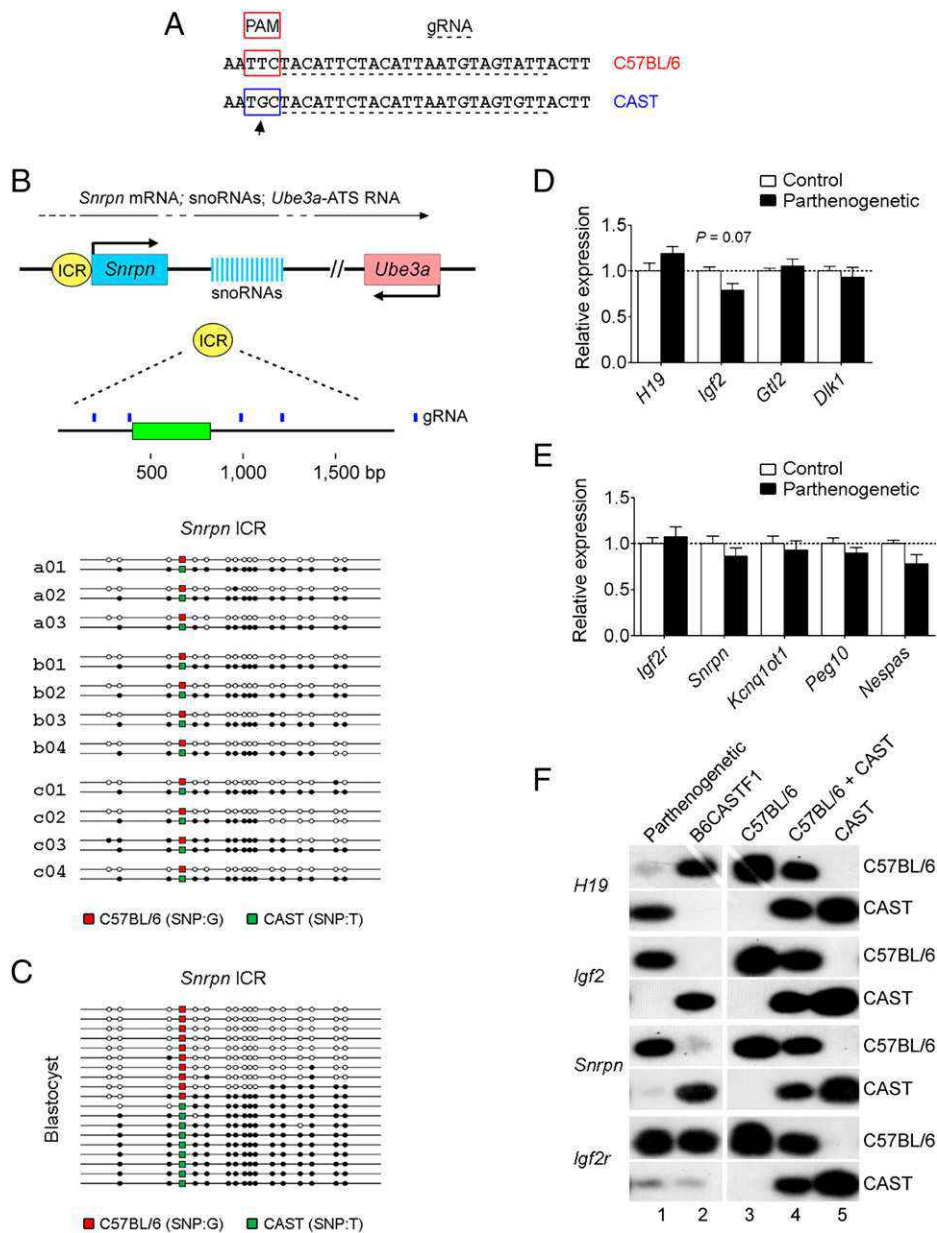
Wei et al.
Viable offspring derived from single unfertilized mammalian oocytes

PNAS | 3 of 7
https://doi.org/10.1073/pnas.2115248119

Fig. 2. Targeted methylation rewriting of five maternally methylated ICRs in parthenogenetic embryos. (*A*) Strategy to target one allele but not the other. The sgRNA sequence is underlined. The PAM for sgRNA (TTN) is labeled by a red box. The arrow indicates the SNP (C57BL/6, T; CAST, G). (*B*) Targeted demethylation of the *Snrpn* ICR on the C57BL/6 allele in oocytes. A schematic illustrating the *Snrpn* ICR locus is shown at the top of the panel. The region subjected to methylation analysis is indicated by a green rectangle. The gRNAs are indicated by blue bars. Single MII oocytes were subjected to bisulfite sequencing analysis. Each single-oocyte sample was assigned an ID beginning with a letter, followed by a two-digit number. Different letters represent different oocyte donors, and different numbers distinguish different oocytes from the same donor. White circles represent unmethylated CpGs, and black circles represent methylated CpGs. The polymorphism is indicated with red for G from the C57BL/6 allele and with green for T from the CAST allele. The editing of methylation of four other maternally methylated ICRs—*Igf2r*, *Kcnq1ot1*, *Peg10*, and *Nespas* ICRs—is present in *SI Appendix*, Fig. S8. (*C*) Maintenance of methylation of the *Snrpn* ICR in parthenogenetic preimplantation embryos. The microinjection of RNAs and construction of putatively diploid parthenogenetic embryos were performed as described above. After parthenogenetic activation and in vitro embryonic culture, one-fifth of the converted DNA from ~100 pooled E 3.5 blastocysts was subjected to bisulfite sequencing analysis. The maintenance of methylation of four other ICRs is present in *SI Appendix*, Fig. S9. (*D*) Quantitative real-time PCR analysis of imprinted genes regulated by paternally methylated ICRs in control (white columns) and modified parthenogenetic (black columns) E 9.5 embryos. (*E*) Quantitative real-time PCR analysis of imprinted genes regulated by maternally methylated ICRs in control (white columns) and reconstructed parthenogenetic (black columns) E 9.5 embryos. Control, *n* = 9; parthenogenetic, *n* = 8. The values represent expression levels relative to that of the internal control gene *Gapdh*. Data are expressed as mean ± SEM *P < 0.05, **P < 0.01, versus control. The dotted line (set as 1) represents the average of expression levels of each gene from controls. (*F*) SNuPE assays for allele-specific expression of the indicated genes. Lanes 1 and 2 contained DNA derived from the pooled RNA of reconstructed parthenogenetic and fertilized control E 9.5 embryos, respectively. Lanes 3 and 5 contained DNA derived from the pooled RNA of C57BL/6 and CAST E 9.5 embryos, respectively. Lane 4 contained DNA derived from a 1:1 mixture of RNA from C57BL/6 and CAST E 9.5 embryos.

Table 1. Development of modified parthenogenetic embryos[2 + 5]

Developmental progress	No.
No. of reconstructed oocytes	227
No. of oocytes developed to blastocyst	192 (84.6% of reconstructed oocytes)
No. of embryos transferred	192 (100% of blastocysts)
No. of pregnants/recipients	14/14
No. of live pups	3 (1.6% of embryos transferred to recipients)
No. of survived pups	1 (0.5% of embryos transferred to recipients)

patterns, indicating that the edited methylation marks were inherited to the fully developed organism, which is critical for supporting full-term parthenogenetic development (Fig. 3*B* and *SI Appendix*, Fig. S15*A*). In contrast, bisulfite sequencing of tail tissue from two parthenogenetic mice that died within 24 h of birth demonstrated that at least one of the seven ICRs exhibited loss of methylation imprinting, confirming that all seven ICRs are necessary for full-term development of parthenogenetic mouse embryos

Fig. 3. Generation of parthenogenetic mice by targeted methylation rewriting of seven ICRs. (*A*) Parthenogenetic mice that grew to adulthood with normal reproductive performance. Shown is a photograph of the parthenogenetic mouse ~4.5 mo old and her offspring. (*B*) Bisulfite sequencing of the *H19* ICR and *Peg10* ICR in the live parthenogenetic mouse. The methylation status of five other ICRs of the live parthenogenetic mouse is present in *SI Appendix*, Fig. S15*A*. (*C*) Bisulfite sequencing of the *H19* ICR in one growth-retarded parthenogenetic mouse that was alive at term but died within 24 h. The methylation status of six other ICRs is present in *SI Appendix*, Fig. S15*B*. (*D*) Bisulfite sequencing of the *Peg10* ICR in the other growth-retarded parthenogenetic mouse that was alive at term but died within 24 h. The methylation status of six other ICRs is present in *SI Appendix*, Fig. S15*C*. Abnormal methylation was also observed on the *Snrpn* ICR of this animal. Tail tip DNA was used for methylation analysis. White circles represent unmethylated CpGs, and black circles represent methylated CpGs. The polymorphism is indicated with red from the C57BL/6 allele and with green from the CAST allele.

(Fig. 3 *C* and *D* and *SI Appendix*, Fig. S15 *B* and *C*). We observed that although the one mouse with a normal body weight at birth grew to adulthood, it displayed postnatal growth retardation, with an approximate 19.8% reduction in body weight compared with controls (*SI Appendix*, Fig. S16*A*). This might be explained by the third critical paternally methylated ICR, *Rasgrf1* ICR, which regulates *Rasgrf1* expression and was not edited. *Rasgrf1* regulates postnatal growth by inducing growth hormone secretion from the pituitary gland (24), and in our study, *Rasgrf1* expression was down-regulated in the brains of parthenogenetic mice compared with those of controls (*SI Appendix*, Fig. S16*B*). After mating with a stud male at 16 wk of age, the parthenogenetic mouse showed normal reproductive performance (Fig. 3 *A*). Quantitative real-time PCR of brains derived from three randomly selected pups revealed normal expression levels of *Rasgrf1*, suggesting that the primary imprinting disorder cannot potentially be transmitted to the next generation because of a new round of germline epigenetic reprogramming (*SI Appendix*, Fig. S17).

To further determine whether the unmodified *Rasgrf1* ICR accounts for the postnatal growth retardation observed in parthenogenetic mice, we performed additional methylation editing of this locus. The *Rasgrf1* imprinting cluster contains an ~8-kb paternally methylated ICR (25). We designed eight sgRNAs targeting this locus (*SI Appendix*, Table S2 and Fig. S18*A*). After validation of the effective sgRNAs in oocytes (*SI Appendix*, Fig. S18 *B–D*), we applied them to the construction of parthenogenetic embryos. We constructed parthenogenetic embryos with seven previously mentioned ICRs, together with *Rasgrf1* ICR modification, which we designated parthenogenetic embryos[3 + 5]. The transfer of 155 E 3.5 parthenogenetic embryos[3 + 5] generated two live offspring (*SI Appendix*, Table S3). Both had body weight (1.142 and 1.104 g) similar to that of controls (1.138 ± 0.034 g; mean ± SEM) at birth and survived to adulthood. Both mice exhibited normal methylation patterns at the *Rasgrf1* ICR (*SI Appendix*, Fig. S18*E*). Body weight trajectories showed a body weight gain of both mice comparable to that of wild-type controls (*SI Appendix*, Fig. S18*F*), supporting the hypothesis that the unmodified *Rasgrf1* ICR contributed to the postnatal growth retardation of the parthenogenetic individual.

Together, these data demonstrate that parthenogenesis can be achieved in mammals by appropriate epigenetic regulation of multiple ICRs. This is consistent with the famous parental conflict hypothesis (also known as the Haig hypothesis) (6, 7), which proposes that the imprinting-mediated balance between paternal and maternal genomes is critical for mammalian development.

We considered several possibilities to explain the low efficiency of parthenogenetic mouse generation. First, only a small portion of embryos with all seven imprinting regions corrected can support full-term development. Consistent with this idea, two of six E 13.5 embryos (*SI Appendix*, Fig. S14) and one of three newborn offspring (*SI Appendix*, Fig. S15) exhibited correct methylation imprinting at all seven regions edited. In fact, this may underestimate the frequency of unsuccessfully edited embryos. We speculate that many modified embryos with incorrect imprinting died earlier than E 13.5 or birth. Second, it is possible that we missed additional important loci. One such
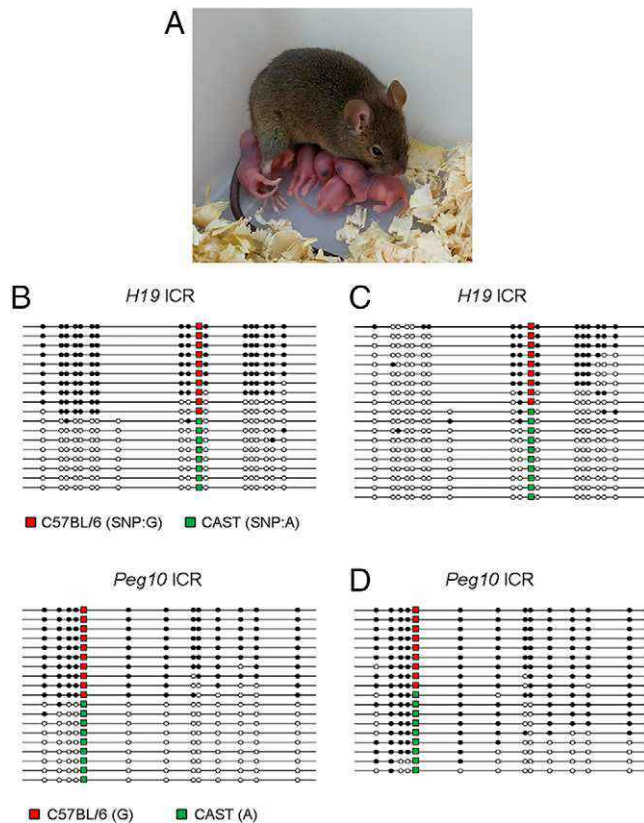
Wei et al.
Viable offspring derived from single unfertilized mammalian oocytes

PNAS | 5 of 7
https://doi.org/10.1073/pnas.2115248119

candidate is *Grb10*, which has been shown to participate in the generation of bipaternal mice (16). Using elegant haploid embryonic stem cell techniques, Li et al. were able to generate both bimaternal and bipaternal mice by genetic modification of multiple imprinting regions, among which *Grb10* is involved in the full-term development of bipaternal embryos (16).

The success of parthenogenesis in mammals opens many opportunities in agriculture, research, and medicine. Further identification and editing of additional ICRs might improve the efficiency of parthenogenetic development. Further optimization of the editing system, such as employment of chimeric Dnmt3a/3l (26) or multiple Dnmt3a domains via the SunTag system (27), might enhance the efficiency of multiple editing and improve the success rate of generation of viable parthenogenetic offspring. Future studies are also required to comprehensively assess off-target problems.

Methods

Mice. All animal care and use procedures were in accordance with guidelines of the Institutional Animal Care and Use Committee. Mice used for oocyte donors were B6CASTF1 (C57BL/6 ♀ × CAST ♂) background, whereas mice used for foster mothers were CD1 background. All mice were housed under controlled temperature (22 ± 2 °C) and lighting (12:12 h light:dark cycle) and had free access to sterile water and pellet food ad libitum.

Generation of dCas9-Dnmt3a and dCpf1-Tet1 mRNA and sgRNA. We introduced the T7 promoter to the targeted sequence by PCR to generate templates used for in vitro transcription. For dCas9-Dnmt3a, the T7 promoter was added by PCR using primer dCas9-Dnmt3a For and Rev (*SI Appendix*, Table S4) and Addgene plasmid 84476 as the template. For the dCas9-Dnmt3a inactive form, the T7 promoter was added by PCR using primer dCas9-Dnmt3a IF For and Rev (*SI Appendix*, Table S4) and Addgene plasmid 84478 as the template. For dCpf1-Tet1 and its mutant, overlap PCR was used to generate the templates (28). For sgRNA coinjected with dCas9-Dnmt3a (or its mutant) mRNA, the T7 promoter was added to specific sgRNAs by PCR using different primers (*SI Appendix*, Table S4) and Addgene plasmid 42230 as the template. For CRISPR RNA (crRNA) coinjected with dCpf1-Tet1 (or its mutant) mRNA, the T7 promoter was added to specific crRNA by PCR using the different primers. Primers used are listed in *SI Appendix*, Table S4. The full-length protein sequences of dCas9-Dnmt3a and dCpf1-Tet1 and their mutants are listed in *SI Appendix*, Table S5. Additional details are provided in *SI Appendix*, SI Methods.

GV Oocyte Collection and Microinjection. Oocytes at the GV stage were used for microinjection. Ovaries were isolated from female B6CASTF1 mice (8–12 wk old) 46 h after intraperitoneal injection of 10 international units (IU) of pregnant mare's serum gonadotrophin, and cumulus oocyte complexes were recovered from ovaries by repeatedly puncturing antral follicles with a fine steel needle under the visual field of a dissecting microscope (29). Cumulus cells were removed by brief treatment with hyaluronidase (3 mg/mL) in M2 medium. The dCas9-Dnmt3a or dCpf1-Tet1 mRNA (50 ng/μL) and sgRNA (20 ng/μL) were injected into the cytoplasm of GV oocytes with a well-recognized GV in M2 medium. Additional details are provided in *SI Appendix*, SI Methods.

Construction of Parthenogenetic Embryos. PB1 was transferred into the cytoplasm of the sibling MII oocyte to form diploid parthenogenetic embryos. Initially, MII oocytes were treated briefly with 5 μg/mL cytochalasin B in M2 medium for ~5 min. Only mature oocytes with intact round PB1 were used for further experiments. PB1 was slowly sucked into the injection pipette with a piezo-driven actuator and was briefly aspirated in and out in 7% polyvinylpyrrolidone until the PB1 membrane broke down slightly. PB1 was then injected into the cytoplasm of sibling MII oocytes. MII oocytes were artificially activated by treatment in Ca^{2+}-free M16 medium containing 10 mM $SrCl_2$ for 2 h. The reconstructed embryos with two second polar bodies and pronuclei were washed and cultured in 50-μL droplets of potassium simplex optimized medium supplemented with amino acids under mineral oil at 37 °C in humidified air containing 5% CO_2 until the blastocyst stage at 3.5 d. Thereafter, 12–16 blastocysts were transferred to the uterine horns of 2.5-d post coitum pseudopregnant recipients (6–8 blastocysts for each uterine horn). Live pups were recovered by autopsy at 19.5 d of gestation.

Bisulfite Sequencing. Bisulfite genomic sequencing was performed as previously described (18). Briefly, for MII oocytes, bisulfite modification was accomplished using a method previously developed in our laboratory (18). A single MII oocyte containing its genetic sibling PB1 was subjected to each reaction. Briefly, tetrahydrofurfuryl alcohol was used to protect the DNA from degradation. A 9-nt adaptor was ligated with the fragmented DNA, and the fragments were amplified three times to generate sufficient templates for PCR amplification. A detailed procedure for single-oocyte–specific region bisulfite sequencing is provided in *SI Methods*. For blastocysts, pooled E 3.5 blastocysts were directly subjected to the EZ DNA Methylation-Direct Kit (Zymo Research) for bisulfite conversion. For E 13.5 embryos or somatic tissues, genomic DNA was purified using the Wizard Genomic DNA Purification Kit (Promega), after which bisulfite modification was accomplished using the EZ DNA Methylation Kit (Zymo Research). The converted DNA was then amplified by PCR with primer sequences as summarized in *SI Appendix*, Table S6. Additional details are provided in *SI Appendix*, SI Methods.

Quantitative Real-Time PCR. We analyzed mRNA levels by qRT-PCR after reverse transcription as described before (30). Total RNA was extracted using the TRIzol reagent (Invitrogen) and quantified by absorbance at 260 and 280 nm in a PerkinElmer spectrophotometer. It was then used as a template for complementary DNA synthesis by SuperScript III first-strand synthesis (Invitrogen) with random hexamers. The mRNA quantity was determined with the qRT-PCR 7500 system (Applied Biosystems), using primer sequences as summarized in *SI Appendix*, Table S7 and SYBR Green SuperMix UDG (Invitrogen). Additional details are provided in *SI Appendix*, SI Methods.

SNuPE. SNuPE was performed as previously described (19, 20). Total RNA from E 9.5 embryos was extracted using TRIzol reagent (Invitrogen) as described above. RT-PCR products were isolated from the agarose gel using the MinElute Gel Extraction Kit (Qiagen). Primers used to distinguish C57BL/6 and CAST alleles were as described by Szabó and Mann (20) and are listed in *SI Appendix*, Table S8. Additional details are provided in *SI Appendix*, SI Methods.

ChIP Assay. We performed ChIP as previously described (31). The antibody used in this experiment is anti-CTCF rabbit polyclonal antibody (07729, Millipore). qPCR primers are listed in *SI Appendix*, Table S9. Additional details are provided in *SI Appendix*, SI Methods.

Statistical Analyses. Data were analyzed by SPSS 16.0 after log transformation or square-root transformation unless raw data were normally distributed. Measurements were analyzed by ANOVA, or, if appropriate, by two-tailed Student's *t* test. All data are shown as mean ± SEM. $P < 0.05$ was considered statistically significant.

Data Availability. All study data are included in the article and/or supporting information.

1. J. McGrath, D. Solter, Completion of mouse embryogenesis requires both the maternal and paternal genomes. *Cell* **37**, 179–183 (1984).
2. M. A. Surani, S. C. Barton, M. L. Norris, Development of reconstituted mouse eggs suggests imprinting of the genome during gametogenesis. *Nature* **308**, 548–550 (1984).
3. T. Kono et al., Birth of parthenogenetic mice that can develop to adulthood. *Nature* **428**, 860–864 (2004).
4. M. Kawahara et al., High-frequency generation of viable mice from engineered bi-maternal embryos. *Nat. Biotechnol.* **25**, 1045–1050 (2007).
5. W. Reik, J. Walter, Genomic imprinting: Parental influence on the genome. *Nat. Rev. Genet.* **2**, 21–32 (2001).
6. D. Haig, Colloquium papers: Transfers and transitions: Parent-offspring conflict, genomic imprinting, and the evolution of human life history. Proc. Natl. Acad. Sci. U. S. A. **107 Suppl 1**, 1731–1735 (2010).
7. T. Moore, D. Haig, Genomic imprinting in mammalian development: A parental tug-of-war. *Trends Genet.* **7**, 45–49 (1991).
8. D. P. Barlow, Genomic imprinting: A mammalian epigenetic discovery model. *Annu. Rev. Genet.* **45**, 379–403 (2011).

6 of 7 | PNAS
https://doi.org/10.1073/pnas.2115248119

Wei et al.
Viable offspring derived from single unfertilized mammalian oocytes

9. J. L. Thorvaldsen, K. L. Duran, M. S. Bartolomei, Deletion of the H19 differentially methylated domain results in loss of imprinted expression of H19 and Igf2. *Genes Dev.* **12**, 3693–3702 (1998).

10. S. P. Lin *et al.*, Asymmetric regulation of imprinting on the maternal and paternal chromosomes at the Dlk1-Gtl2 imprinted cluster on mouse chromosome 12. *Nat. Genet.* **35**, 97–102 (2003).

11. A. Wutz *et al.*, Imprinted expression of the Igf2r gene depends on an intronic CpG island. *Nature* **389**, 745–749 (1997).

12. J. S. Sutcliffe *et al.*, Deletions of a differentially methylated CpG island at the SNRPN gene define a putative imprinting control region. *Nat. Genet.* **8**, 52–58 (1994).

13. G. V. Fitzpatrick, P. D. Soloway, M. J. Higgins, Regional loss of imprinting and growth deficiency in mice with a targeted deletion of KvDMR1. *Nat. Genet.* **32**, 426–431 (2002).

14. C. M. Williamson *et al.*, Identification of an imprinting control region affecting the expression of all transcripts in the Gnas cluster. *Nat. Genet.* **38**, 350–355 (2006).

15. R. Ono *et al.*, Deletion of Peg10, an imprinted gene acquired from a retrotransposon, causes early embryonic lethality. *Nat. Genet.* **38**, 101–106 (2006).

16. Z. K. Li *et al.*, Generation of Bimaternal and Bipaternal Mice from Hypomethylated Haploid ESCs with Imprinting Region Deletions. *Cell Stem Cell* **23**, 665–676.e4 (2018).

17. Z. Li *et al.*, Birth of fertile bimaternal offspring following intracytoplasmic injection of parthenogenetic haploid embryonic stem cells. *Cell Res.* **26**, 135–138 (2016).

18. Y. Wei *et al.*, DNA methylation analysis and editing in single mammalian oocytes. *Proc. Natl. Acad. Sci. U.S.A.* **116**, 9883–9892 (2019).

19. J. Singer-Sam, Quantitation of specific transcripts by RT-PCR SNuPE assay. *PCR Methods Appl.* **3**, S48–S50 (1994).

20. P. E. Szabó, J. R. Mann, Allele-specific expression and total expression levels of imprinted genes during early mouse development: Implications for imprinting mechanisms. *Genes Dev.* **9**, 3097–3108 (1995).

21. A. C. Bell, G. Felsenfeld, Methylation of a CTCF-dependent boundary controls imprinted expression of the Igf2 gene. *Nature* **405**, 482–485 (2000).

22. C. M. B. A. Williamson *et al.*, *MRC Harwell* (World Wide Web Site - Mouse Imprinting Data and References, Oxfordshire, 2013).

23. B. Zetsche *et al.*, Cpf1 is a single RNA-guided endonuclease of a class 2 CRISPR-Cas system. *Cell* **163**, 759–771 (2015).

24. S. J. Clapcott, J. Peters, P. C. Orban, R. Brambilla, C. F. Graham, Two ENU-induced mutations in Rasgrf1 and early mouse growth retardation. Mammalian *Genome* **14**, 495–505 (2003).

25. T. Watanabe *et al.*, Role for piRNAs and noncoding RNA in de novo DNA methylation of the imprinted mouse Rasgrf1 locus. *Science* **332**, 848–852 (2011).

26. P. Stepper *et al.*, Efficient targeted DNA methylation with chimeric dCas9-Dnmt3a-Dnmt3L methyltransferase. *Nucleic Acids Res.* **45**, 1703–1713 (2017).

27. C. Pflueger *et al.*, A modular dCas9-SunTag DNMT3A epigenome editing system overcomes pervasive off-target activity of direct fusion dCas9-DNMT3A constructs. *Genome Res.* **28**, 1193–1206 (2018).

28. K. L. Heckman, L. R. Pease, Gene splicing and mutagenesis by PCR-driven overlap extension. *Nat. Protoc.* **2**, 924–932 (2007).

29. B. Hogan, F. Costantini, E. E. Lacy, *Manipulating the Mouse Embryo: A Laboratory Manual* (Cold Spring Harbor Laboratory Press, 1994).

30. Y. Wei *et al.*, Paternally induced transgenerational inheritance of susceptibility to diabetes in mammals. *Proc. Natl. Acad. Sci. U.S.A.* **111**, 1873–1878 (2014).

31. M. F. Carey, C. L. Peterson, S. T. Smale, Chromatin immunoprecipitation (ChIP). Cold Spring Harbor *Protocols* **2009**, pdb prot5279 (2009).

DEVELOPMENTAL BIOLOGY